Journal of Applied Mechanics and Technical Physics, Vol. 35, No. 6, 1994

UNIFORM DEFORMATION OF A GRANULAR MEDIUM. THEORY AND EXPERIMENT

D. Kolymbas, S. V. Lavrikov, and A. F. Revuzhenko

UDC 539.3

The solution of most continuum mechanics problems requires the selection or the creation of a mathematical model of the medium. If we are talking about an elastic body or a linearly viscous fluid, the model construction problem does not exist, since the classical models have been created and the corresponding Lamé and Navier–Stokes equations have been formulated. For the more complex media, for example the elastoplastic and granular media and the nonlinear fluids, there are no generally accepted equations. Therefore the model selection question must be resolved separately for the problems of each class. Here much depends on the specific conditions of loading and the objectives which are posed in formulating and solving the specific problems [1].

Practically all the continuum working models are of a phenomenological nature. This means that they are constructed on the basis of some fundamental experiments. These experiments must determine both the constructive equations themselves and the values of the parameters appearing in these equations.

The question of selection of the basis experiments is far from simple. In principle, any experiments, for example the penetration of dies, can be used to construct the mathematical models. However, for the interpretation of this experiment it is necessary to select in advance the mathematical model, solve the boundary-value problem, compare the results with the experimental data, correct the model, and so on. This is a very complex procedure. However, there is a special class of loadings for which preliminary data on the mathematical model are not required for the interpretation of the experiment. This is the class of quasi-static loadings, in which the distributions of the stresses and the strains in space are uniform. Here the deformation process reduces to the realization of a sequence of affine transformations. Therefore, in the stable processes the kinematics of the deformation will be the same for both the elastoplastic media and for the viscous or any other media. Thus, the experiments that realize the uniform states are ideal as the basis experiments for the construction and analysis of the mathematical models of continuous media.

It is not technically possible to achieve precisely uniform loading. Therefore the most that we can do is to realize deformation processes that are as close to uniform as is possible. Such processes and the corresponding techniques are well known for the metals [2, 3]. These include the twisting and stretching of thin-wall tubular specimens. However, this classical technique is not applicable for the granular media, liquids with complex rheology, and other such materials. Here it is necessary to seek new fundamental experiments.

A general classification of the uniform deformation processes is given in [4, 5]. In this classification the well-known processes appear as particular cases: uniform tension, torsion, and so on. But, in spite of the near triviality of the problem formulation, new classes of loadings have been found. Several devices and instruments for realizing the fundamental experiments have been developed on the basis of these new classes [6-9].

In the present work the results obtained in [6-9] for granular materials are used to analyze the hypoplastic model [10-12].

1. The constitutive relations model, connecting the stress tensor T and the strain rate tensor D, have the form

$$\overset{\circ}{T} = \left(C_1 \mathrm{tr}(T)D + C_2 \frac{\mathrm{tr}(TD)}{\mathrm{tr}(T)} T + (C_3 T^2 + C_4 T^{*2}) \frac{I_s\sqrt{\mathrm{tr}(D^2)}}{\mathrm{tr}(T)}\right) I_s,$$
$$\dot{e} = (1 + e)\mathrm{tr}(D), \tag{1.1}$$

Novosibirsk, Russia. Karlsruhe, Germany. Translated from Prikladnaya Mekhanika i Tekhnicheskaya Fizika, No. 6, pp. 114-121, 1994. Original article submitted February 4, 1994.

0021-8944/94/3506-0920$12.50

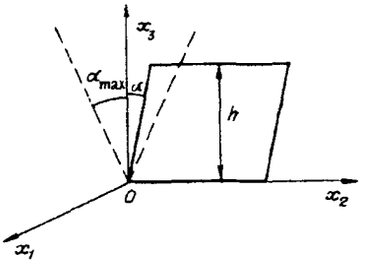

Fig. 1

where

$$I_e = (1 - a)\frac{e - e_{min}}{e_{kr} - e_{min}} + a;\ I_s = 1 + \exp\left(-r_1\frac{e - e_{min}}{e_{kr} - e_{min}}\right);$$
$$a = 1 + q_2\exp(-q_3|\mathrm{tr}(T)|),\ e_{kr} = p_1 + p_2\exp(-p_3|\mathrm{tr}(T)|); \tag{1.2}$$

$\mathring{T} = \dot{T} - WT + TW$ is the Jaumann derivative of the tensor T; $W = 0.5(\nabla\bar{v} - \nabla\bar{v}^T)$ is the distortion tensor; $\bar{v}$ is the velocity vector; e is the porosity of the medium; $T^* = T - \mathrm{tr}(T)E/3$; and E is the unit tensor. The constants of the material (obtained for dry Karlsruhe (FRG) sand) are as follows:

$$C_1 = -33.5,\ C_2 = -341.4,\ C_3 = -339.7,\ C_4 = 446.5,\ r_1 = 35.0, e_{min} = 0.4,$$
$$p_1 = 0.47,\ p_2 = 0.47,\ p_3 = 0.00018kPa,\ q_2 = -0.25,\ q_3 = 0.0001kPa. \tag{1.3}$$

The model (1.1)-(1.3) makes it possible to describe both the active loading state and the unloading process using the same equations. Therefore the nonlinear nature of the model is retained upon conversion to the increments.

2. We shall examine the pure shear process as the first basic experiment. A uniform shear device was created for the realization of this experiment under laboratory conditions [6, 7]. This device is a cubic chamber that can experience shears while its volume remains unchanged (Fig. 1, view from above: the square transforms to a parallelogram without change of the height).

The experiments were performed as follows. We selected the initial chamber configuration (the initial shear angle), poured the material into the chamber, and performed the shearing. After a definite time the direction of shearing was reversed. We measured the shear angle α and the change of the height of the material specimen in the chamber ΔH. Since the chamber base area is unchanged, the ratio $\Delta H/H$ coincides with the relative change of the volume, i.e., it characterizes the dilatancy of the specimen. In the experiments we also measured the shears σ_{ij} with a floating pickup, located at a definite depth within the specimen. The results were published in [6, 7].

Now let us perform numerical experiments using an analogous loading scheme for the model (1.1)-(1.3). Let $Ox_1x_2x_3$ be the Cartesian coordinate system (see Fig. 1) and shearing be realized in the plane Ox_2x_3. To the uniform deformation field in the plane Ox_2x_3 there will correspond the velocities

$$v_2 = 2sx_3,\ v_3 = 0,$$
$$s = \pm k - \text{const},\ k > 0, \tag{2.1}$$

where the symbols $\pm$ indicate the direction of shearing.

We shall isolate a horizontal layer at a definite depth from the free surface of the material. In the experiments it was verified that the friction of the material against the side walls of the chamber can be neglected because of the dilatancy of the material. Therefore the vertical load acting on the layer can be considered to be constant and equal to the weight of the overlying layers (in Figs. 2b-d, 4b-d, 6b-d, 7b-d the stress corresponding to this load is shown by the dashed lines):

$$\sigma_{11} = C,\ \text{or}\ \dot{\sigma}_{11} = 0. \tag{2.2}$$

The condition of uniformity of the deformation for the selected horizontal layer has the form $\partial v_1/\partial x_2 = \partial v_1/\partial x_3 = 0$ and closes the system of equations (1.1)-(1.3), (2.1), (2.2). For the field (2.1) the tensors D and W take the form

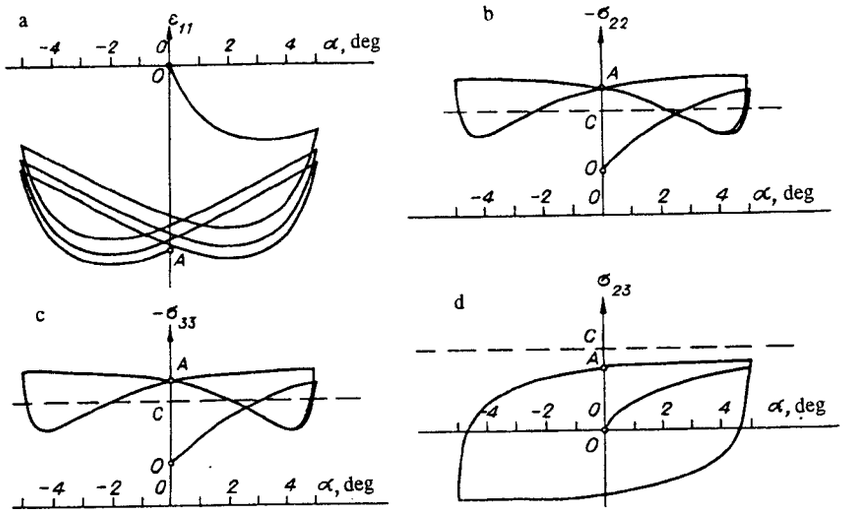

Fig. 2

$$D = \begin{vmatrix} d & 0 & 0 \\ 0 & 0 & s \\ 0 & s & 0 \end{vmatrix}, \quad W = \begin{vmatrix} 0 & 0 & 0 \\ 0 & 0 & s \\ 0 & -s & 0 \end{vmatrix},$$

where $d = \dot{\varepsilon}_{11} = \partial v_1/\partial x_1$. The quantity d characterizes uniquely the dilatancy.

Thus, the problem reduces to the solution of the tensor equations (1.1)-(1.3) with the conditions (2.1), (2.2). In componentwise form they represent a system of ordinary first-order differential equations with nonlinear right side. This system is solved numerically by the Euler method on a computer. We shall describe the results.

We specify at the initial moment of time the following initial state of the medium:

$$\sigma_{11} = C = \text{const}, \sigma_{22} = \sigma_{33} = \xi C, \sigma_{12} = \sigma_{13} = \sigma_{23} = 0,$$
$$\varepsilon_{ij} = 0, i,j = \overline{1.3}, e = 0{,}7, \xi = 0.42 \tag{2.3}$$

(ξ is the coefficient of lateral thrust). The chamber shape is uniquely characterized by the angle α, which we shall use as the loading parameter (see Fig. 1). We specify at the initial moment $\alpha = \alpha_0$ and select some maximal angle α_{max}. We perform the loading as follows: shearing is first accomplished in the positive direction from the angle α_0 to α_{max} (s = k). After this the direction of shearing is reversed (s = −k), and shearing is realized from the angle α_{max} to the angle $-\alpha_{max}$. Then shearing takes place from the angle $-\alpha_{max}$ to α_{max}, and so on. For (2.3) we take $\alpha_0 = 0$, $\alpha_{max} = 5°$.

The calculations show that during deformation the volume of the material in the chamber changes from cycle to cycle, i.e., the medium dilates. This is clearly seen on the graph of the dependence of the magnitude of the vertical deformation ε_{11} on the shearing angle α (Fig. 2,a), here and in the sequel the point O corresponds to the beginning of deformation, and the point A corresponds to the end of deformation. We see that in the case of cyclic shear loading constant maximal angle α_{max} the material compacts in the course of time. Initially the porosity e = 0.7 (point O), at point A is e = 0.665. The medium compaction process slows from cycle to cycle. The calculations show that after a certain number of cycles this process exhausts itself, i.e., the dilatancy curve approaches the stationary regime. In the stationary regime the entire deformation history is forgotten, and all the parameters depend only on the phase within the cycle.

The graphs of the stresses σ_{22}, σ_{33}, σ_{23} are shown in Figs. 2b-d, respectively. We see that all the stresses also approach the stationary regime. It is interesting to note that the cyclic variation of the stresses σ_{22},σ_{23} in the stationary regime takes place around the value C, while at the initial moment of time $\sigma_{22} = \sigma_{33} = \xi C$, $\xi = 0.42$. In other words, shearing in a granular medium in a certain sense "relieves" the internal friction, and the medium approaches with respect to its properties a Pascal-law fluid.

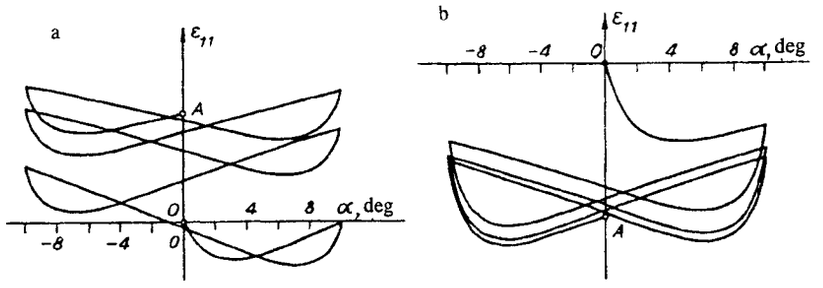

Fig. 3

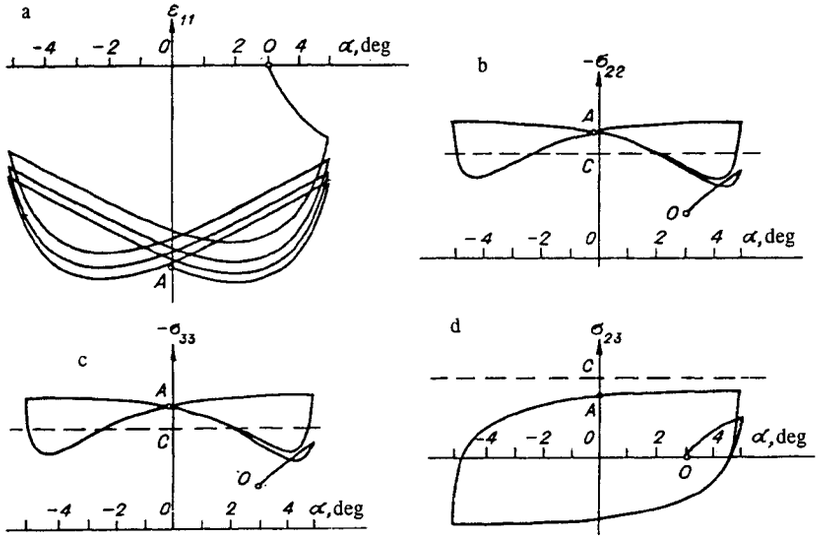

Fig. 4

The obtained results were compared with the experimental results of [6, 7]. The conclusions that were drawn for the model (1.1)-(1.3) that the granular medium in the case of cyclic shearing dilates and that in the course of time this process stabilizes and the lateral stresses σ_{22}, σ_{33} acquire values that are close to the vertical stress σ_{11} are fully confirmed by the experiments.

Further, the experiments of [6, 7] show that upon approach to the stationary regime the dependence of all the parameters on the shearing amplitude α_{max} remains the same. Namely: if after reaching the stationary regime we change α_{max}, then the stationarity is disrupted and a definite number of cycles is again required for stabilization of the deformation. The new stationary state will differ from the preceding stationary state. Thus, if we increase the angle α_{max}, this will lead to decompaction of the material in comparison with the preceding state. Conversely, reduction of the angle α_{max} leads to compaction. This is a general property for the various granular materials, and it must be described by the mathematical model. We shall verify its satisfaction for the model (1.1)-(1.3).

We take all the problem parameters to be the same as in the preceding example except for the maximal angle α_{max}. We set $\alpha_{max} = 10°$ and perform the calculations. The results with respect to the dilatancy are shown in Fig. 3a. As we would expect, increase of the angle α_{max} led to decompaction of the material: the porosity at point A is e = 0.745 (in the preceding example the final porosity is e = 0.665). We also see from Fig. 3a that the decompaction process slows in the course of time, and the deformation process finally stabilizes.

The experiments of [6, 7] also show that the dilatancy depends on the magnitude of the preload on the surface of the granular medium. If we preload the material on the surface, then after reaching the stationary state the packing of the particles will be more dense than if the same experiment is performed without preloading. In the numerical experiment the preloading can be modeled as follows. We take the initial stresses to be three times greater than in the preceding examples,

i.e., $\sigma_{11} = 3C$, $\sigma_{22} = \sigma_{33} = 3\xi C$. We set the maximal angle $\alpha_{max} = 10°$ and take the remaining parameters from (2.3). The calculations show that introduction of the preload leads to compaction of the material even with the shearing amplitude $\alpha_{max} = 10°$ (Fig. 3,b). If the initial porosity e = 0.7, then at the point A e = 0.668.

All the foregoing calculation examples relate to the case when the initial shearing angle $\alpha_0 = 0$. The properties of the granular medium are such [6, 7] that the initial angle σ_0 influences only the first few deformation cycles. In this case the very fact of approach to the stationary regime and the values of all the parameters are independent of α_0. In other words, in the granular medium the information on the initial state is quickly "forgotten." This is one of the basic properties of the media of this type. We shall verify its satisfaction for the model (1.1)-(1.3). We take the problem parameters from (2.3) and set $\alpha_0 = 3°$. The calculations show that the initial phase has an influence only in the very beginning of deformation. After one or two cycles the dilatancy (Fig. 4a) and the stresses (Fig. 4b-d) do not differ significantly from the analogous parameters that are calculated with $\alpha_0 = 0$ (Fig. 2a-d).

For the model (1.1)-(1.3) the directions of the principal axes of the stress tensor can be calculated from the values of the stresses σ_{22}, σ_{33}, σ_{23}. The calculations show that the principal axes of the stress tensor form an angle of $\pm$ 44.625° to the axis Ox_2; this agrees fully with the experiments in the limits of their accuracy.

3. The foregoing calculations relate to the case of simple loading. However, for the analysis of the mathematical models the situations are also of interest when the uniform state is realized with complex loading with rotation of the principal axes of the stresses. A technique for the realization of such loading was proposed in [8]. For this we must give the material specimen the form of an elliptical cylinder and specify on the boundary in the plane Ox_2x_3 conditions of the form

$$\mathbf{w} \cdot \mathbf{n} = 0, \ \mathbf{w} \times \mathbf{r} = \Omega = \text{const}, \tag{3.1}$$

where $\mathbf{w} = \{v_1, v_2, v_3\}$ is the velocity vector; $\mathbf{r} = \{0, x_2, x_3\}$ is the radius-vector; $\mathbf{n} = \{0, n_2, n_3\}$ is the vector of the normal to the elliptical boundary of the specimen (Fig. 5). The conditions (3.1) mean that all the points of the elliptical boundary travel along the boundary with constant sectorial velocity. In this case the distribution of the deformations will be uniform, and therefore an experiment that is close to (3.1) can be used as the basis experiment [9].

Experimental data on the complex loading of a granular medium with rotation of the principal axes of the stress tensor were presented in [9]. We shall now perform numerical experiments on the model (1.1)-(1.3) with the conditions on the boundary (3.1). By virtue of the uniformity of the deformations, the following velocity distribution is realized in the specimen:

$$v_2 = \Omega x_3 / b^2, \ v_3 = -\Omega x_2 / a^2. \tag{3.2}$$

Here a, b are the semi-axes of the ellipse ($a > b$); $\Omega = \text{const}$ ($\Omega > 0$ corresponds to counterclockwise motion).

We take the scheme of the numerical calculations to be the same as in the case of shearing without rotation of the axes. As before, we shall determine the vertical component v_1 of the velocity from the loading condition (2.2) and the uniformity conditions $\partial v_1/\partial x_2 = \partial v_1/\partial x_3 = 0$. The tensors D and W for the field (3.2) have the form

$$D = \begin{vmatrix} d & 0 & 0 \\ 0 & 0 & p \\ 0 & p & 0 \end{vmatrix}, \quad W = \begin{vmatrix} 0 & 0 & 0 \\ 0 & 0 & -q \\ 0 & q & 0 \end{vmatrix},$$

where $p = \Omega(a^2 - b^2)/(2a^2b^2)$; $q = \Omega(a^2 + b^2)/(2a^2b^2)$; $d = \dot{\varepsilon}_{11} = \partial v_1/\partial x_1$. Here, just as in the preceding case, the elliptical chamber section area is invariable. Therefore d characterizes uniquely the dilatancy of the layer. We shall describe the results.

We take the following initial state of the medium:

$$\begin{gathered} \sigma_{11} = C = \text{const}, \ \sigma_{22} = \sigma_{33} = \xi C, \ \sigma_{12} = \sigma_{13} = \sigma_{23} = 0, \\ \varepsilon_{ij} = 0, \ i,j = \overline{1,3}, \ \xi = 0.42, \ e = 0.85. \end{gathered} \tag{3.3}$$

We shall perform the loading as follows. We specify a definite value of the velocity Ω. We fix some material point of the elliptical boundary. We shall use as the loading parameter the angle α, by which the radius-vector of the point, drawn from the center of the ellipse, rotates. We shall increase α from 0 to some fixed value, for example, 10π.

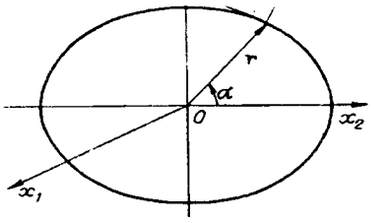

Fig. 5

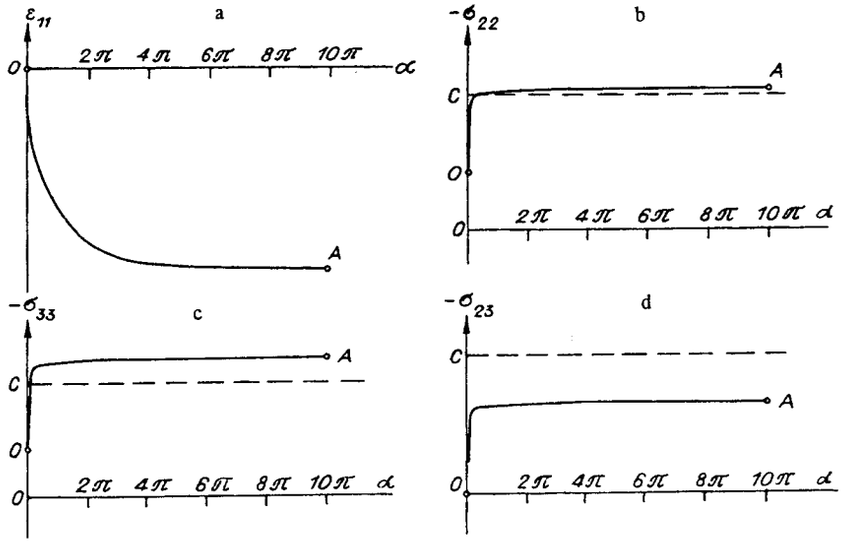

Fig. 6

The calculations made using the described loading scheme show good agreement with the laboratory experiment results. It was found that here, just as in the experiments, the material in the elliptical chamber dilates (compacts) during deformation. In the course of time this process stabilizes and approaches the stationary regime, when the values of all the parameters do not change upon further deformation. The graph of the dependence of the deformation ε_{11} on the angle α is shown in Fig. 6a: at point O the porosity e = 0.85, at point A e = 0.783. Figures 6b-d show the graphs of the stresses σ_{22}, σ_{33}, σ_{23}. We see that the changes of the stresses in the course of time also approach the stationary regime, practically in a single revolution (change of α by 2π). The compressive stress σ_{33} on a small area with its normal along the minor axis of the ellipse is higher than the stress σ_{22} on a small area with its normal along the major axis.

One of the basic questions in the complex loading case is the orientation of the principal stress axes. In the experiments of [9] for a granular material it was found that the principal axes of the stress tensor coincide in the plane Ox_2x_3 with the axes of the ellipse. The largest compressive stress is directed along the minor axis of the ellipse, and the smallest is directed along the major axis. In other words, in this situation the condition of coaxiality of the stress tensor and the strain tensor is approximately satisfied. In the numerical experiment for the model (1.1)-(1.3) these axes are observed to differ by an angle of 41.24°. The principal axes of the stress tensor and of the strain rate tensor differ by an angle of 3.76°. The calculated values of the magnitudes of the principal stresses are close to the experimental values. The question of the degree of misalignment of the stress tensor, the strain tensor, and the strain rate tensor in the case of loadings with rotations of the axes requires further study.

We shall now alter the loading scheme and examine the situation when the direction of rotation can change in the loading process. We set e = 0.75 and take the remaining values of the parameters from (3.3). We perform the numerical loading using the following scheme. We first increase the angle α from 0 to 2π. Then we change the direction of rotation and reduce α from 2π to π. Then we again change the direction and perform the loading from $\alpha = \pi$ to $\alpha = 2\pi$. The calculations show the following. Change of the direction of loading leads to marked compaction of the material with subsequent

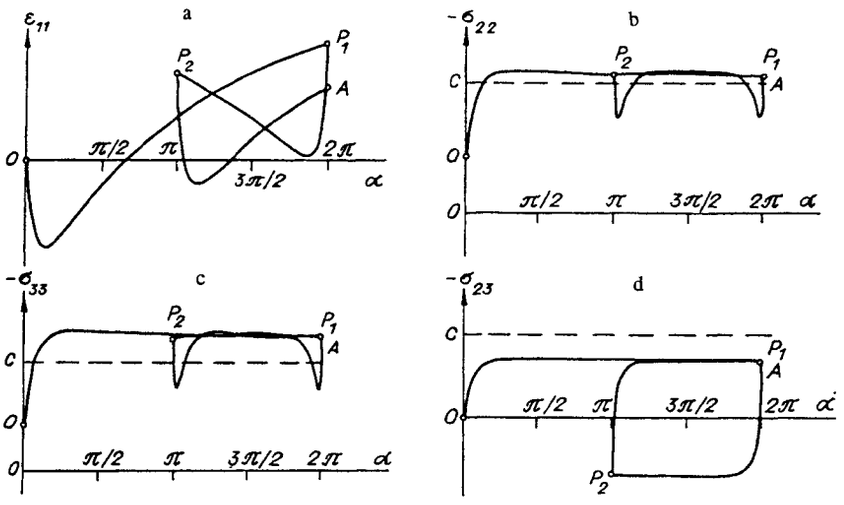

Fig. 7

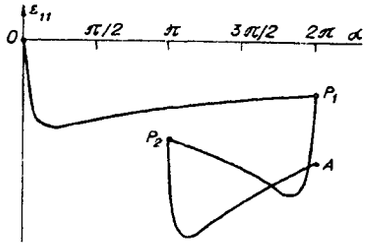

Fig. 8

stabilization of the deformation (Fig. 7a, here and in the following the loading curve is OP_1P_2A). At point O, the porosity e = 0.75, at point A, e = 0.764. This result agrees completely with the experiments of [9], where it was shown that high density of the material can be achieved with cyclic change of the direction of the load with small amplitudes of the angle α. The graphs of the stresses σ_{22}, σ_{33}, σ_{23} are shown, respectively, in Figs. 7b-d. We see from these graphs that change of the direction of loading leads to a jump of the stresses, but after this the deformation process rapidly stabilizes.

We shall consider still another calculation example. We take all the values of the parameters from (3.3) and double the initial stresses: $\sigma_{11} = 2C$, $\sigma_{22} = \sigma_{33} = 2\xi C$ (account for preloading). We can expect that this will lead to more dense packing of the particles of the medium in all the stages of deformation. The calculations showed that stabilization actually does take place with a higher density of the medium (Fig. 8) than in the example without preloading. The initial porosity at point O, e = 0.75, the final porosity at point A, e = 0.724.

Thus, 1) the technique and experiments of [6-9] can be used as the basis for the construction and analysis of the mathematical models of the deformation of complex media, 2) the hypoplastic model of the granular medium [10-12] correctly predicts correctly a whole series of subtle deformation effects and can be used for the solution of boundary problems.

REFERENCES

1. V. V. Novozhilov, "Two articles on mathematical models in continuum mechanics," Preprint, IPM AN SSSR, LGU, No. 225, Moscow (1983).
2. A. M. Zhukov and Yu. N. Rabotnov, "Study of plastic deformations of steel under complex loading," Inzh. Sb., No. 18 (1954).
3. A. A. Il'yushin and V. S. Lenskii, Resistance of Materials [in Russian], Fizmatgiz, Moscow (1959).

4. A. F. Revuzhenko, "On very simple continuum flows," Dokl. Akad. Nauk SSSR, Vol. 303, No. 1 (1988).
5. A. F. Revuzhenko, "Experimental detection of constitutive behavior and self-organization," in: Modern Approaches to Plasticity, Elsevier, Amsterdam (1993).
6. A. F. Revuzhenko, S. B. Stazhevskii, and E. I. Shemyakin, "On the deformation mechanism of a granular material with large shears," Fiz.-Tekh. Probl. Razab. Polez. Iskop. No. 3 (1974).
7. A. P. Bobryakov and A. F. Revuzhenko, "Uniform shear of a granular material. Dilatancy," Fiz.-Tekh. Probl. Razab. Polez. Iskop. No. 5 (1982).
8. A. F. Revuzhenko, "A class of complex loadings of an inelastic medium," Prikl. Mekh. Tekh. Fiz. No. 5 (1986).
9. A. P. Bobryakov and A. F. Revuzhenko, "On a method for testing inelastic materials," Izv. Akad. Nauk SSSR. Mekh. Tverd. Tela, No. 4 (1990).
10. D. Kolymbas, "Generalization of the hypoplastic constitutive equation," in: Proc. Constitutive Equations for Granular Noncohesive Soils, (1989), pp. 349-366.
11. D. Kolymbas and W. Wu, "Introduction to hypoelasticity," in: Modern Approaches to Plasticity, Elsevier, Amsterdam (1993).
12. E. Bauer and W. Wu, A Hypoplastic Model for Granular Soils under Cyclic Loading, Elsevier, Amsterdam (1993).